



Al-Mg systematics of CAIs, POI, and ferromagnesian chondrules from Ningqiang

Weibiao HSU^{1,2}, Gary R. HUSS³, and G. J. WASSERBURG^{1*}

¹The Lunatic Asylum, Division of Geological & Planetary Sciences 170–25, Caltech, Pasadena, California 91125, USA

²Purple Mountain Observatory, Chinese Academy of Sciences, 2 West Beijing Road, Nanjing, 210008, China

³Department of Geological Sciences and Center for Meteorite Studies, Arizona State University, Tempe, Arizona 85287–1404, USA

*Corresponding author. E-mail: isotopes@gps.caltech.edu

(Received 20 February 2002; revision accepted 1 November 2002)

Abstract—We have made aluminum-magnesium isotopic measurements on 4 melilite-bearing calcium-aluminum-rich inclusions (CAIs), 1 plagioclase-olivine inclusion (POI), and 2 ferromagnesian chondrules from the Ningqiang carbonaceous chondrite. All of the CAIs measured contain clear evidence for radiogenic $^{26}\text{Mg}^*$ from the decay of ^{26}Al ($\tau = 1.05$ Ma). Although the low Al/Mg ratios of the melilites introduce large uncertainties, the inferred initial $^{26}\text{Al}/^{27}\text{Al}$ ratios for the CAIs are generally consistent with the value of 5×10^{-5} . There is clear evidence of $^{26}\text{Al}^*$ in one POI and two chondrules, but with considerable uncertainties in the value of $(^{26}\text{Al}/^{27}\text{Al})_0$. The $(^{26}\text{Al}/^{27}\text{Al})_0$ ratios for the POI and the chondrules are $0.3\text{--}0.6 \times 10^{-5}$, roughly an order of magnitude lower than the canonical value. Ningqiang shows very little evidence of metamorphism as a bulk object and the $(^{26}\text{Al}/^{27}\text{Al})_0$ ratios in its refractory inclusions and chondrules are consistent with those found in other unmetamorphosed chondrites of several different classes. Our observations and those of other workers support the view that ^{26}Al was widely and approximately homogeneously distributed throughout the condensed matter of the solar system. The difference in $(^{26}\text{Al}/^{27}\text{Al})_0$ between CAIs and less refractory materials seems reasonably interpreted in terms of a ~ 2 million year delay between the formation of CAIs and the onset of formation of less refractory objects. The POI shows clear differences in $^{25}\text{Mg}/^{24}\text{Mg}$ between its constituent spinels and olivine, which confirms that they are partially reprocessed material from different sources that were rapidly quenched.

INTRODUCTION

We report an isotopic study of aluminum-magnesium systematics of calcium-aluminum-rich inclusions (CAIs), plagioclase-olivine inclusions (POIs), and ferromagnesian chondrules from the Ningqiang carbonaceous chondrite. Since the initial discovery of live ^{26}Al ($\tau = 1.05$ Ma) in Allende (Lee, Papanastassiou, and Wasserburg 1976, 1977), widespread evidence of ^{26}Al has been found in a variety of chondritic material including CAIs, POIs, and chondrules of various types in carbonaceous and ordinary chondrites (Hutcheon and Hutchison 1989; Sheng, Hutcheon, and Wasserburg 1991; MacPherson, Davis, and Zinner 1995; Russell et al. 1996; Kita et al. 2000; Hsu, Wasserburg, and Huss 2000; Huss et al. 2001). Based on the widespread occurrence of a maximum $^{26}\text{Al}/^{27}\text{Al}$ value in CAIs, a canonical value of $^{26}\text{Al}/^{27}\text{Al} \sim 5 \times 10^{-5}$ has been established for the ^{26}Al abundance in the early solar system. Many CAIs from carbonaceous, ordinary, and enstatite chondrites have inferred initial ratios, $(^{26}\text{Al}/^{27}\text{Al})_0$, that are very close to the

canonical value; others have distinctly lower ratios (cf., MacPherson, Davis, and Zinner 1995; Russell et al. 1996; Guan et al. 2000; Huss et al. 2001). The search for evidence of live ^{26}Al in objects other than CAIs has been less successful. For the few POIs and chondrules from carbonaceous and ordinary chondrites exhibiting evidence of radiogenic ^{26}Mg ($^{26}\text{Mg}^*$), the inferred $(^{26}\text{Al}/^{27}\text{Al})_0$ fall below the canonical value by factors of 5 to 100 (Sheng, Hutcheon, and Wasserburg 1991; Srinivasan, Huss, and Wasserburg 2000; Kita et al. 2000; Huss et al. 2001). It follows that CAIs and chondrules are sampling different populations of “nebular” materials in terms of their ^{26}Al abundances. The differences in $(^{26}\text{Al}/^{27}\text{Al})_0$ have been interpreted to indicate the time interval between the formation of CAIs and chondrules, or to reflect the effects of parent-body metamorphism on these objects. It is possible that this difference may reflect a very heterogeneous distribution of ^{26}Al throughout the nebula. As part of our continuing effort to constrain the abundance and distribution of ^{26}Al in the early solar system, we carried out an ion probe study of magnesium isotopic compositions of 4

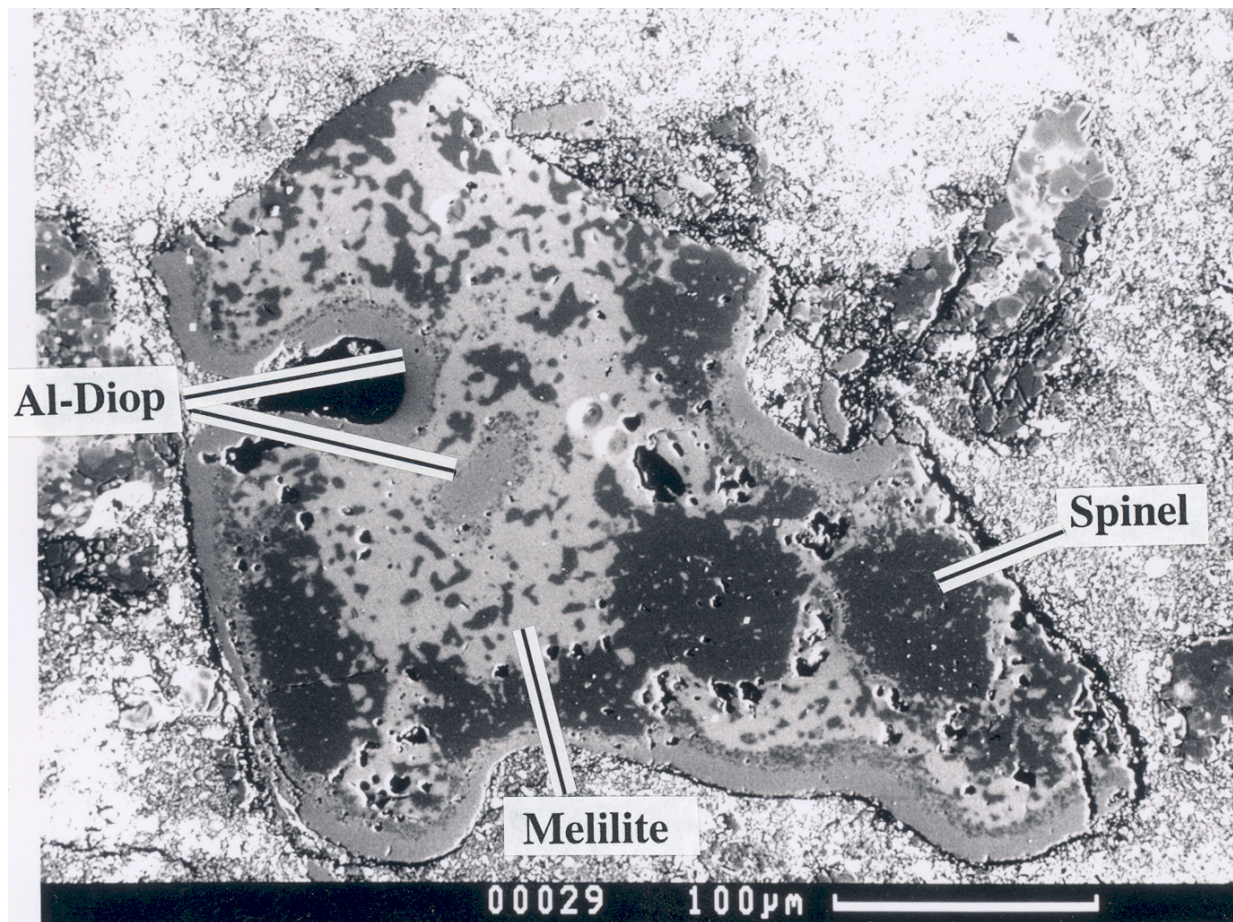


Fig. 1. Backscattered electron images of CAI-1 in Ningqiang. Much of its interior consists of melilite (45 vol%) that encloses irregular clusters of small spinel grains. Note that a large spinel patch occurs near the rim of the inclusion. More than half of its outer surface is rimmed by a 15 μm layer of aluminous diopside (Al-diopside, 20 vol%). Near the center of the inclusion, there is a small patch of Al-diopside ($10 \times 20 \mu\text{m}$), which is possibly part of the rim.

melilite-bearing CAIs, one POI, and 2 olivine chondrules from the Ningqiang meteorite. A preliminary report of this work was presented by Hsu, Huss, and Wasserburg (1999).

This paper is intended to be a short report of our observations on ^{26}Al systematics in Ningqiang. In presenting this data, we consider that any meteorite is a mixture of objects from different sources and with different histories. The meteorite itself is a small sample of part of a parent planetary body. After its assembly, this body has been subjected to metamorphism of varying degrees in different locations within that body. The parent body was subsequently disrupted, generating the meteorite. When we consider the metamorphism of the meteorite, we refer to those metamorphic episodes after the meteorite was last assembled from its constituent components. After assembly, these components will all have undergone a common level of metamorphism, and it is this metamorphism that is referred to in the text. If there are fine-grained phases present in the meteorite that preserve evidence of ^{26}Al , we do not consider that the meteorite could have undergone a high level of

metamorphism after it was assembled. The origins of various constituent lithic components in the meteorite (e.g., CAIs, chondrules, matrix, etc.) have never been elucidated and we do not propose specific mechanisms of formation here. The isotopic heterogeneities (e.g., magnesium isotopic shifts between phases) are preserved from before the aggregation of the meteorite. The source of one of these shifts, attributed to ^{26}Al decay, is the main focus of this report.

Ningqiang has been classified as an anomalous carbonaceous chondrite (Rubin et al. 1988; Weisberg et al. 1996). It shares many characteristics with oxidized CV3 meteorites. Petrographically, Ningqiang closely resembles Allende (CV3), having numerous large ($>1 \text{ mm}$) and well-defined chondrules surrounded by an abundant matrix ($\sim 50\%$) of fine-grained fayalitic olivine. However, its bulk oxygen isotopic composition is somewhat more ^{16}O -rich than Allende (Weisberg et al. 1996), it is less enriched in refractory lithophiles ($\sim 1.21 \times \text{CI}$) than CV chondrites ($\sim 1.35 \times \text{CI}$), and it has higher abundances of volatile elements and carbon than CV chondrites (Rubin et al. 1988; Kallemeyn 1996). The

refractory inclusions in Ningqiang are less abundant (1 vol%) and smaller (~300 μm) than those of other CV3s. In this study, we found four melilite-bearing CAIs with sizes from 200 to 700 μm .

The search for evidence of live ^{26}Al in chondrules is hampered by two difficulties. First, technical limitations require that measurements be made on mineral phases with high Al/Mg ratios to permit detection of small enrichments in $^{26}\text{Mg}/^{24}\text{Mg}$. Secondly, most chondrules contain few minerals with high Al/Mg. Earlier studies of aluminum-magnesium isotopic systematics in chondrules have focused on relatively rare aluminum-rich chondrules, which are more likely to contain phases with high Al/Mg (cf., Russell et al. 1996; Srinivasan, Huss, and Wasserburg 2000; Huss et al. 2001). It was assumed that aluminum-rich chondrules were closely related to the more common ferromagnesian chondrules and thus could serve as analog materials. Recently, $^{26}\text{Mg}^*$ has been detected in ferromagnesian chondrules from unequilibrated ordinary chondrites (UOCs) (Kita et al. 2000; McKeegan et al. 2000; Mostefaoui et al. 2002). The data collected to date show that chondrules with widely varying chemical compositions from UOCs have similar aluminum-magnesium isotopic systematics. In Ningqiang, we found two ferromagnesian chondrules containing aluminum-rich glasses. These glasses have Al/Mg ratios of up to 100 and are good candidates for ion probe measurements. We sought to establish if these magnesium-rich chondrules share similar $(^{26}\text{Al}/^{27}\text{Al})_0$ ratios with the aluminum-rich chondrules measured in Allende and other carbonaceous chondrites.

EXPERIMENTAL PROCEDURES

All samples studied are in 1 inch round, polished thin sections. They are Ningqiang W(164)5, W(164)6, W(164)7, W(164)8, and LC419. The samples were first studied with a petrographic microscope and interesting areas were photographed and characterized using a JEOL JSM-35CF scanning electron microscope (SEM) equipped with a Tracor Northern energy dispersive (EDS) x-ray analysis system. CAIs were located by x-ray mapping.

Magnesium isotopic measurements were carried out with PANURGE, a modified CAMECA IMS-3f ion probe, using an O^- primary beam. The beam current used was 0.05 to 1 nA, which resulted in a beam spot diameter on the sample of 1 to 5 μm . The details of the method were described by Fahey et al. (1987). A mass resolving power of 3000 was used, which is sufficient to remove hydride and other interferences. A liquid nitrogen trap was used near the secondary ion source to further depress the hydride signal. The count rates ^{24}Mg , ^{25}Mg , and ^{26}Mg were kept under $2 \times 10^5 \text{ s}^{-1}$, 10^4 s^{-1} , and 10^4 s^{-1} , respectively, to reduce the deadtime correction. The uncertainty in the deadtime was typically 1 nanosecond. Standards of Burma spinel, San Carlos olivine, melilite glass, Miakajima plagioclase, and Cr-diopside were analyzed periodically during sample

measurements with the PANURGE. The respective Al/Mg sensitivity factor ratios were determined by comparing electron probe and ion probe data. Intrinsic Mg isotopic mass fractionation for different minerals was determined by comparing the $^{25}\text{Mg}/^{24}\text{Mg}$ ratios measured for each sample mineral with the ratios measured for the equivalent terrestrial mineral standard as monitored during a run. The fractionation of $^{25}\text{Mg}/^{24}\text{Mg}$ is given by:

$$F_{\text{Mg}} = \Delta^{25}\text{Mg}(\text{sample}) - \Delta^{25}\text{Mg}(\text{standard}) \quad (1)$$

where

$$\Delta^{25}\text{Mg} = \left(\frac{(^{25}\text{Mg}^+ / ^{24}\text{Mg}^+)_{\text{MEAS}}}{(^{25}\text{Mg} / ^{24}\text{Mg})_{\text{REF}}} - 1 \right) \times 1000(\text{‰}) \quad (2)$$

where $(^{26}\text{Mg}/^{24}\text{Mg})_{\text{REF}} = 0.13932$ and $(^{25}\text{Mg}/^{24}\text{Mg})_{\text{REF}} = 0.12663$ are from Catanzaro et al. (1966).

To determine whether there was any ^{26}Mg excess ($^{26}\text{Mg}^*$) due to the decay of ^{26}Al , a linear fractionation law was assumed for both the instrumental and intrinsic magnesium-isotope mass fractionation, and the mass-fractionation-corrected, non-linear ^{26}Mg excess in per mil was calculated from the following equation:

$$\delta^{26}\text{Mg} = \left[\frac{(^{26}\text{Mg}/^{24}\text{Mg})}{0.13932} \left(1 - 2 \frac{\Delta^{25}\text{Mg}}{10^3} \right) - 1 \right] \times 10^3 \quad (3)$$

Instrumental fractionation for Burma spinel, San Carlos olivine, melilite glass, Cr-diopside, and Miakajima plagioclase are -8.1 ± 0.3 , -4.7 ± 0.3 , -3.8 ± 0.4 , and $-1.3 \pm 0.5 \text{ ‰/amu}$ respectively, and their corresponding $\delta^{26}\text{Mg}$ are 0.8 ± 1.0 , 0.3 ± 1.0 , 0.7 ± 1.0 , 0.4 ± 1.0 , and $0.6 \pm 1.2\text{‰}$ (2σ). The fractionation values reported for each phase were obtained taking into account the fractionation factors determined for each reference standard mineral as monitored during the sample run.

PETROGRAPHY

We studied 4 melilite-bearing CAIs, 1 POI, and 2 ferromagnesian chondrules.

Calcium-Aluminum-Rich Inclusions

CAI-1 is a coarse-grained melilite-spinel inclusion. It is a convoluted, irregularly-shaped CAI fragment about $300 \times 300 \mu\text{m}$ in size (Fig. 1). Much of its interior consists of melilite (45 vol%) that encloses irregular clusters of small spinel grains. Large spinel patches (35 vol%) up to 50 μm across also occur, often near the rim of the inclusion. More than half of its outer surface is rimmed by a 15 μm layer of aluminous diopside (20 vol%). Near the center of the inclusion, there is a small patch of aluminous diopside ($10 \times 20 \mu\text{m}$), which is possibly part of the rim.

CAI-2 is a triangle-shaped, melilite-bearing CAI

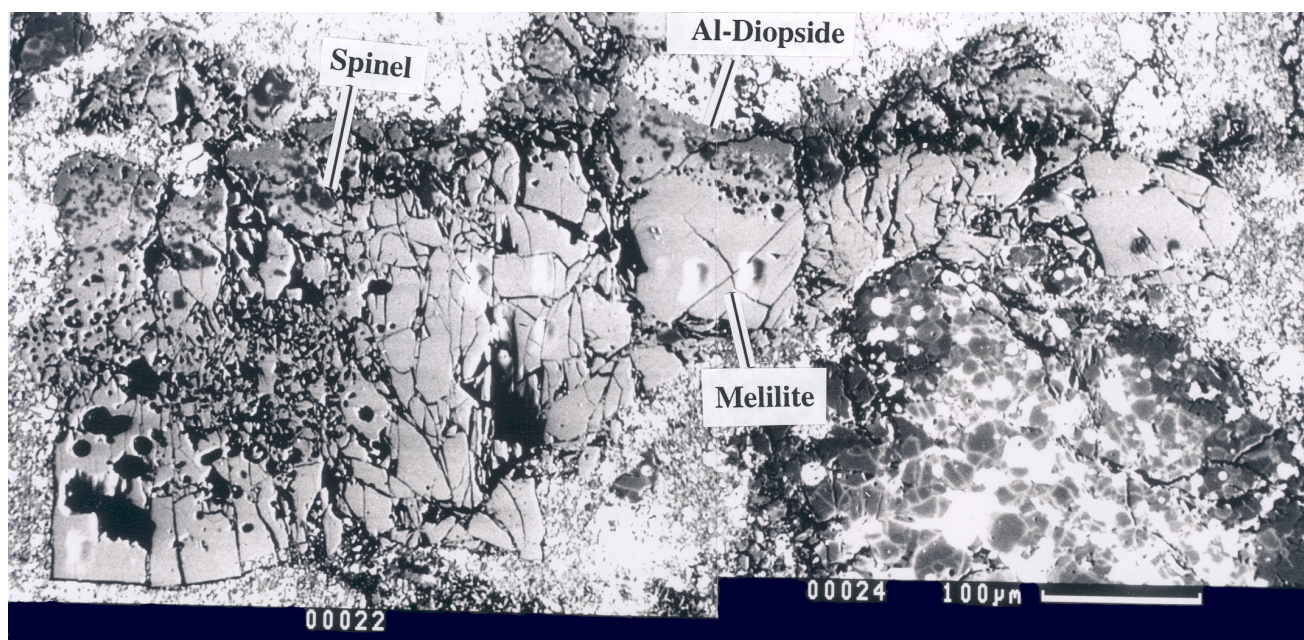


Fig. 2. Backscattered electron image of CAI-2 in Ningqiang. It is a fragment of a melilite-bearing CAI consisting of melilite, Al-diopside, and spinel. The melilite grains are well-crystallized (up to 100 μm) and free of diopside and spinel inclusions. Diopside and spinel mainly occur on one side of the fragment. Al-rich diopside forms a 10 μm layer on the edge and beneath this layer small μm -sized spinel grains are scattered within a zone of 20 to 50 μm . This region may represent the rim of the original inclusion before it was fragmented.

fragment, about 200 \times 700 μm in size (Fig. 2). It mainly consists of melilite (85 vol%), aluminous diopside (10 vol%), and spinel (5 vol%). The melilite grains are well formed (up to 100 μm) and free of diopside and spinel inclusions. Diopside and spinel mainly occur on one side of the fragment. Aluminous diopside forms a 10 μm layer on the edge. Beneath this layer, small μm -sized spinel grains are scattered within a zone of 20 \times 50 μm . This region may represent the rim of the original lithic inclusion before it was fragmented.

CAI-3 is also a melilite-bearing inclusion. It is an elongated CAI with a size of 200 \times 500 μm . The interior part is mainly melilite (50 vol%) that encloses diopside (40 vol%) and spinel grains (10 vol%). There is a large spinel patch (50 μm) inside the inclusion. This CAI is also partially rimmed by a 10 μm layer of aluminous diopside.

CAI-4 is an irregularly-shaped inclusion. It has a loose texture and contains 80 vol% aluminous diopside, 15 vol% melilite, and 5 vol% spinel. Fine-grained spinel and melilite (\sim 10 μm) are enclosed by Al-diopside. Much of the inclusion is rimmed by aluminous diopside.

Plagioclase-Olivine Inclusion

The POI is a 2.6 \times 3.0 mm ovoid object first described by Rubin et al. (1988) and later studied by Lin and Kimura (1997). Readers are referred to Fig. 6b of Rubin et al. (1988) and to Fig. 2 of Lin and Kimura (1997) for more detailed petrological descriptions. The inclusion is dominated by

anorthite (An_{80-94}) with lesser amounts of spinel and forsterite ($\text{Fo}_{>99}$). Anorthite crystals are up to 500 μm long and 200 μm wide and often polysynthetically twinned. They contain numerous inclusions of spinel, usually small (\sim 5 μm) and rounded, which is suggestive of resorption. Spinel inclusions tend to be clustered locally in anorthite crystals. Olivine often occurs interstitially between anorthite grains. The inclusion has a 1 mm thick outer region which is mainly composed of coarse euhedral anorthite laths (\sim 500 μm) and olivine grains (up to 250 μm). Beneath this layer is a fine-grained olivine and spinel mantle. The inclusion has a core of coarse-grained anorthite laths.

Ferromagnesian Chondrules

Chon-1 is a round, compound, olivine chondrule (\sim 3 mm in diameter). The interior (\sim 1.5 mm) is mainly made of porphyritic olivine grains up to 500 μm in size (Fig. 3a). Between the olivine grains is a mesostasis of feldspathic glass (areas up to \sim 50 μm across, Fig. 3b). This glass has Al/Mg ratios up to 100. The outer part of the chondrule is composed of two hemispherical fragments of a barred olivine chondrule that is about 1.5 mm in original diameter. Interstitial to the olivine bars are laths of feldspathic glasses that are 25 μm wide.

Chon-2 is a round barred olivine chondrule (\sim 1.5 mm in diameter). Olivine bars (\sim 50 μm wide) are set in feldspathic glass. These glasses have a spread in chemical composition and can have Al/Mg up to 100. The outer part of the

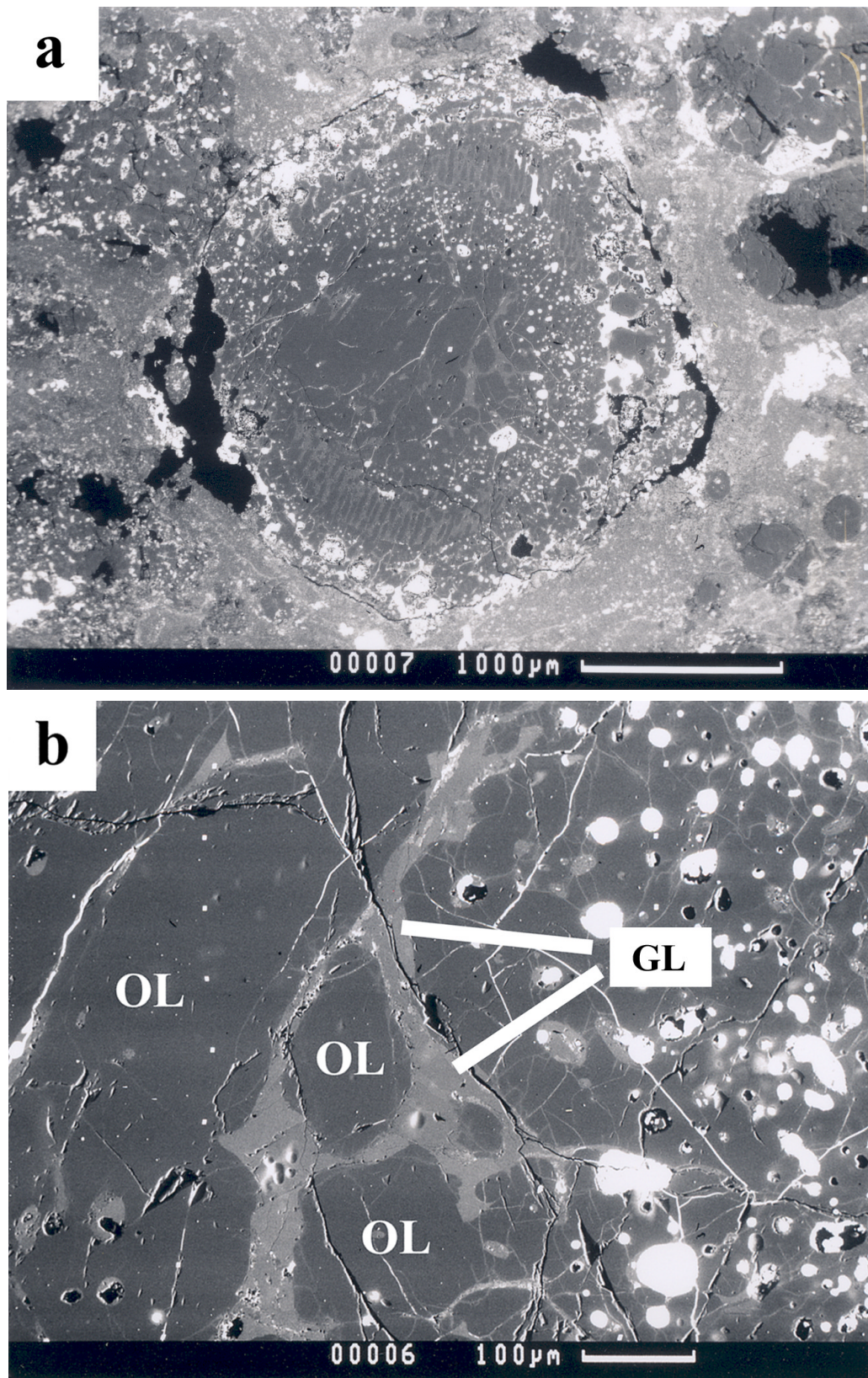


Fig. 3. Backscattered electron image of Chon-1 in Ningqiang. This is a round compound forsterite chondrule (~3 mm in diameter): a) The interior (~1.5 mm) is mainly made of porphyritic olivine grains with sizes of up to 400 μm; b) Between the olivine grains (OL), there are several feldspathic glasses (GL).

chondrule is composed of olivine grains in which are dispersed numerous Fe/FeS blebs (~50 μm), while the central part (~700 μm) is nearly metal- and sulfide-free.

RESULTS

The results of mass fractionation (F_{Mg}), ^{26}Mg excesses, and $^{27}\text{Al}/^{24}\text{Mg}$ ratios in the different mineral phases of the samples are reported in Table 1.

Calcium-Aluminum-Rich Inclusions

Melilites exhibit clear excesses of ^{26}Mg (Table 1), which we believe to be from ^{26}Al . The slope of a regression line through the data on a $^{26}\text{Mg}/^{24}\text{Mg}$ versus $^{27}\text{Al}/^{24}\text{Mg}$ plot (Fig. 4) gives the initial $^{26}\text{Al}/^{27}\text{Al}$ ratio, $(^{26}\text{Al}/^{27}\text{Al})_0$, at the time the object formed (Lee, Papanastassiou, and Wasserburg 1977; Wasserburg and Papanastassiou 1982). Precise determination of $(^{26}\text{Al}/^{27}\text{Al})_0$ requires that objects have phases with high $^{27}\text{Al}/^{24}\text{Mg}$. For objects with potential $(^{26}\text{Al}/^{27}\text{Al})_0$ of 5×10^{-5} , phases with $^{27}\text{Al}/^{24}\text{Mg} > 20$ are desired in the ion probe measurements. In this study, several CAIs have maximum $^{27}\text{Al}/^{24}\text{Mg}$ ratios less than 10, so that the inferred $(^{26}\text{Al}/^{27}\text{Al})_0$ values are subject to large uncertainties.

Melilite in CAI-1 has relatively high $^{27}\text{Al}/^{24}\text{Mg}$ ratios (up to 30). All three measurements exhibit clear evidence of $^{26}\text{Mg}^*$ (up to 12.7‰), and these $^{26}\text{Mg}^*$ excesses are well correlated with $^{27}\text{Al}/^{24}\text{Mg}$. Spinel and diopside in this inclusion have low $^{27}\text{Al}/^{24}\text{Mg}$ ratios (<3) and their magnesium isotopic compositions are indistinguishable from those of the terrestrial standards. A linear regression of data on diopside, spinel, and melilite gives $(^{26}\text{Al}/^{27}\text{Al})_0$ of $(6.1 \pm 1.6) \times 10^{-5}$ (2σ) for this inclusion (Fig. 4a). This ratio is indistinguishable from the canonical value established for the solar nebula.

Melilites in CAI-2, CAI-3, and CAI-4 have rather low $^{27}\text{Al}/^{24}\text{Mg}$ ratios (≤ 10). Melilite in all of these inclusions shows clear ^{26}Mg excesses (up to ~5‰) in spite of low $^{27}\text{Al}/^{24}\text{Mg}$ ratios. The excesses generally correlate with $^{27}\text{Al}/^{24}\text{Mg}$. Spinel and diopside in these objects have normal magnesium isotopic compositions. The inferred $(^{26}\text{Al}/^{27}\text{Al})_0$ for these inclusions are $(5.4 \pm 3.0) \times 10^{-5}$, $(8.6 \pm 2.4) \times 10^{-5}$, and $(6.0 \pm 3.8) \times 10^{-5}$ respectively (Fig. 4). The evidence for ^{26}Al is clear in these samples, but the estimates of $(^{26}\text{Al}/^{27}\text{Al})_0$ have large uncertainties (see Fig. 4). They are broadly consistent with the 5×10^{-5} value.

In two CAIs, CAI-3 and CAI-4, melilite shows small (<6‰) fractionation favoring heavy magnesium isotopes ($F_{\text{Mg}} \approx 3.7 \pm 2.4$ and 4.1 ± 1.0 ‰/amu, respectively). Spinel and diopside of CAI-3 are unfractionated ($F_{\text{Mg}} \approx -0.3 \pm 1.9$ and 0.2 ± 0.4 ‰/amu, respectively). Diopside of CAI-4 may be slightly enriched in light isotopes ($F_{\text{Mg}} \approx -2.3 \pm 0.7$ ‰/amu). All phases in CAI-1 and CAI-2 have essentially unfractionated magnesium. The apparent fractionation found

in magnesium for the melilites relative to the spinel and diopside appears to reflect a complex multistage history. This observation is not easily explained.

Plagioclase-Olivine Inclusion

The POI is a critical sample, where anorthite has Al/Mg ratios up to 100 (Fig. 5a). Because of their relatively large size (up to several hundred μm), multiple analyses were performed in each single anorthite crystal. The anorthite grains analyzed were located both in the outer region as well as the inner region of the inclusion. We found no systematic difference in the characteristics of these grains in terms of Al/Mg ratios or of magnesium isotopic compositions. All crystals have variable Al/Mg ratios and different degrees of $^{26}\text{Mg}^*$, varying from normal to clear ^{26}Mg enrichment (up to 5‰) (Fig. 5a). The weighted mean of all analyses for anorthite is $\delta^{26}\text{Mg} = 2.3 \pm 0.5\%$, which is clearly resolved from the terrestrial standard by more than 8σ (Fig. 5b). We also analyzed olivine grains adjacent to anorthite grains and spinel inclusions within anorthite crystals. All olivine and spinel grains have $^{26}\text{Mg}/^{24}\text{Mg}$ values of the terrestrial standards. The inferred $(^{26}\text{Al}/^{27}\text{Al})_0 = (0.46 \pm 0.16) \times 10^{-5}$, which is an order of magnitude lower than 5×10^{-5} , is very close to the values previously found in POIs from Allende and Axtell (Sheng, Hutcheon, and Wasserburg 1991; Srinivasan, Huss, and Wasserburg 2000). The evidence for excess ^{26}Mg is clear. However, we cannot demonstrate that the data set defines a true isochron.

The mineral phases appear to show different degrees of mass fractionation. Anorthite exhibits a relatively large range in F_{Mg} (Table 1), but with large errors due to counting statistics and is thus quite uncertain. The mean value of F_{Mg} is 0.4 ± 4.7 ‰/amu. Olivine is essentially unfractionated ($F_{\text{Mg}} = 1.6 \pm 1.8$ ‰/amu). However, spinel is consistently enriched in heavy isotopes (4 to 7 ‰/amu for individual measurements) with an average F_{Mg} of 5.4 ± 2.4 ‰/amu. Again the differences in fractionation require a complex formation history. The spinel grains may be relicts from an earlier formation process as found by Sheng, Hutcheon, and Wasserburg (1991).

Ferromagnesian Chondrules

The feldspathic glasses in chondrules Chon-1 and Chon-2 have $^{27}\text{Al}/^{24}\text{Mg}$ ratios up to 100. These glasses show variable $^{26}\text{Mg}/^{24}\text{Mg}$ ratios, ranging from normal up to 5‰ excesses of ^{26}Mg . Fig. 6c is a histogram of $\delta^{26}\text{Mg}$ values for all measurements with $^{27}\text{Al}/^{24}\text{Mg} > 60$ for Chon-1. Six of eight of these measurements give positive ^{26}Mg values, although the individual measurements are not clearly resolvable from normal. However, the weighted mean of these glass analyses is $\delta^{26}\text{Mg} = 2.9 \pm 1.7\%$ (2σ), which appears to be resolved from the normal value. Fig. 6d shows

Table 1. Mg-Al isotopic data of Ningqiang. Errors reported are 2σ of mean. Errors on Al/Mg combine experimental statistical fluctuations with a measurement of the variability of relative elemental sensitivity from run to run, estimated from data acquired for standard minerals. F and $\delta^{26}\text{Mg}$ are in ‰/amu and ‰, respectively.

	F_{Mg}	$\delta^{26}\text{Mg}$	$\frac{^{27}\text{Al}}{^{24}\text{Mg}}$		F_{Mg}	$\delta^{26}\text{Mg}$	$\frac{^{27}\text{Al}}{^{24}\text{Mg}}$		F_{Mg}	$\delta^{26}\text{Mg}$	$\frac{^{27}\text{Al}}{^{24}\text{Mg}}$
CAI-1				Chon-1				POI			
Spinel	1.0±0.8	0.6±1.6	2.5±.01	Olivine	-2.2±0.7	0.4±1.5	0	Spinel	4.5±0.9	-0.6±1.9	2.9±0.1
Diopside	-0.4±2.1	-0.2±2.0	0		-1.5±0.4	0.0±0.9	0		4.7±1.2	-0.8±2.6	4.4±0.2
Melilite	-1.4±2.0	7.1±4.5	17.9±1		-2.9±0.4	-0.2±0.9	0		4.6±1.3	-0.6±2.7	2.6±0.1
	0.1±1.8	12.5±4.3	29.2±1.5	Glass	0.4±3.5	3.0±7.7	67±3		4.6±1.2	-0.4±2.7	2.5±0.1
	-0.1±0.9	12.7±4.3	29.7±1.5		1.8±2.5	-1.0±5.2	67±3		3.8±1.3	0.0±2.7	2.5±0.1
CAI-2					-2.1±2.9	3.9±6.0	81±4		6.4±1.1	1.7±2.3	3.6±0.1
Spinel	1.3±0.8	0.7±1.7	2.5±0.1		1.7±2.7	0.0±5.6	71±4		6.3±1.1	1.6±2.3	3.6±0.1
	2.1±0.9	0.9±1.8	2.5±0.1		-2.1±2.7	2.4±5.7	70±4		6.8±1.2	1.3±2.5	3.8±0.2
Melilite	0.3±1.1	4.5±2.3	9.5±0.5		-0.7±2.0	4.2±4.0	60±3		7.1±1.2	1.9±2.5	4.0±0.2
	0.6±1.1	3.6±2.2	9.3±0.5		-1.2±1.9	3.5±3.3	67±3	Anorthite	1.0±2.6	1.9±5.4	84±4
	-0.2±1.2	3.9±2.4	9.9±0.5		-0.4±1.9	3.7±2.3	26±1		0.8±2.1	2.1±4.1	84±4
	1.1±0.9	2.5±1.9	8.3±0.4		-1.9±2.5	4.5±4.1	59±3		0.0±1.7	3.5±3.2	41±2
	1.5±1.1	1.1±2.3	9.3±0.5		-0.1±2.5	-0.5±4.1	44±2		0.8±2.1	-0.4±4.4	85±4
	1.6±0.9	1.5±1.9	7.1±0.4	Chon-2					-3.5±2.0	3.4±3.7	58±3
	1.5±0.8	2.9±1.6	7.0±0.4	Olivine	-0.4±0.5	-0.5±1.1	0		-1.7±1.8	4.1±3.6	59±3
	0.6±1.0	2.6±2.0	9.8±0.5		-1.6±0.4	0.3±0.8	0		-3.2±1.7	2.8±3.3	52±3
	-0.1±0.9	5.1±1.9	9.7±0.5		-1.6±0.6	0.2±1.2	0		-4.5±1.7	2.7±3.6	62±3
CAI-3				Glass	1.4±1.4	2.6±2.2	35±2		-2.8±1.8	2.0±3.3	67±3
Spinel	0.5±0.9	1.2±1.9	2.9±0.1		-1.3±1.7	-1.8±3.1	75±4		1.0±2.2	1.4±4.5	100±5
	-0.9±0.8	1.9±1.7	2.9±0.1		-2.0±1.8	3.2±3.3	97±5		-1.7±2.2	1.5±4.4	96±5
Diopside	0.4±0.8	0.9±1.7	0.5±0.1		-4.0±2.0	2.5±4.0	103±5		0.5±1.7	3.8±3.6	85±4
	0.2±0.7	-0.2±1.2	0.9±0.1		-2.2±2.2	1.4±3.2	45±2		-2.7±2.2	5.1±3.2	73±4
	0.1±0.7	-0.6±1.4	1.0±0.1		-0.3±2.3	2.1±3.7	84±4		-2.1±2.2	3.8±3.4	70±4
Melilite	3.6±1.1	2.4±2.3	5.6±0.3		-0.4±2.6	-0.1±4.5	102±5		-3.8±2.1	2.5±2.9	76±4
	2.7±1.2	3.3±2.7	8.6±0.4		-0.8±2.2	-2.0±3.4	16±1		-3.6±2.2	1.2±3.4	63±3
	2.1±1.1	4.0±2.4	7.6±0.4		2.1±2.1	0.0±3.1	20±1		0.2±2.3	1.3±3.6	71±4
	5.6±1.4	1.0±3.0	5.1±0.3		-2.7±2.4	0.0±4.2	96±5		3.7±1.7	-0.9±3.6	80±4
	2.6±0.7	3.5±1.4	6.4±0.3		-5.0±2.5	5.1±4.3	101±5		0.2±1.4	2.7±2.7	52±3
	3.1±0.8	3.6±1.6	5.6±0.3		-4.7±2.4	5.0±3.8	102±5		2.0±1.8	3.5±3.6	75±4
	5.2±0.9	4.3±2.0	7.0±0.3		-0.3±2.5	3.1±4.4	92±5		2.5±1.4	1.2±2.8	72±4
	5.4±1.2	6.1±2.5	8.9±0.4	POI					1.5±1.6	3.1±3.1	73±4
	3.6±0.9	0.8±1.8	4.4±0.2	Olivine	2.0±0.9	-0.6±2.0	0		1.6±1.6	3.0±3.1	68±4
	3.4±0.9	2.9±1.8	4.6±0.2		0.6±0.9	-0.4±1.9	0		1.5±1.4	2.8±2.7	64±3
	3.9±0.8	2.0±1.7	4.8±0.2		2.6±1.1	0.0±2.2	0		2.5±1.4	1.1±2.7	56±3
	5.1±0.8	1.8±1.8	4.8±0.2		1.0±1.0	-0.1±2.1	0		2.9±1.5	1.1±3.0	65±3
CAI-4					1.7±1.0	1.1±2.3	0		4.2±1.8	0.3±3.8	69±3
Diopside	-2.3±0.9	0.3±1.8	0.1±0.1		0.6±0.9	-0.5±1.9	0		3.6±2.1	1.1±4.4	69±4
	-2.4±1.0	1.6±2.0	0.1±0.1		3.1±0.9	-0.7±1.8	0		1.3±1.5	2.8±3.1	70±4
Melilite	4.1±1.1	2.6±2.6	6.6±0.3		-0.1±2.7	-0.2±5.6	0		1.0±1.3	1.0±2.5	52±3
	3.6±1.0	4.1±2.2	7.0±0.3		1.2±1.6	-0.4±3.5	0.1±0.1		-1.1±1.2	0.0±2.3	44±2
	4.0±0.8	2.4±1.6	4.2±0.2		1.6±1.5	0.0±3.8	0.1±0.1		3.5±1.5	2.4±3.0	67±3
	3.7±1.0	3.9±2.0	5.8±0.3		1.9±1.1	0.0±2.4	0.2±0.1		1.8±1.3	2.8±2.8	67±3
	3.5±0.9	3.4±1.8	5.5±0.3		2.2±1.4	0.1±3.0	0.2±0.1		1.8±1.4	2.1±3.0	68±3
	4.0±1.0	3.1±2.1	5.5±0.3						-1.4±1.4	5.1±2.9	68±3
	4.8±0.9	3.0±1.9	5.0±0.3						-0.7±1.5	4.5±3.2	71±4
	4.7±0.8	3.1±1.6	4.1±0.2								

similar data for Chon-2 for measurements with $^{27}\text{Al}/^{24}\text{Mg} > 80$. Again, six of eight measurements give positive $\delta^{26}\text{Mg}$ values and the weighted mean of these analyses is $\delta^{26}\text{Mg} = 2.7 \pm 1.4\text{‰}$ (2σ). In both chondrules, the major phase, olivine, has a normal magnesium isotopic composition (Table 1). Although the correlation between $^{26}\text{Mg}^*$ and Al/Mg is not very clear (Figures 6a, b), we consider that these chondrules appear to show resolved excesses of ^{26}Mg compared to terrestrial magnesium that can reasonably be attributed to the

decay of ^{26}Al . The inferred $(^{26}\text{Al}/^{27}\text{Al})_0$ for these chondrules are $(0.64 \pm 0.36) \times 10^{-5}$ and $(0.34 \pm 0.21) \times 10^{-5}$, respectively, far lower than $\sim 5 \times 10^{-5}$, but consistent with previously reported data for Mg-rich and Al-rich chondrules (Russell et al. 1996; Srinivasan, Huss, and Wasserburg 2000; Kita et al. 2000; McKeegan et al. 2000; Huss et al. 2001; Mostefaoui et al. 2002). Neither chondrule shows resolvable mass-fractionation effects in magnesium.

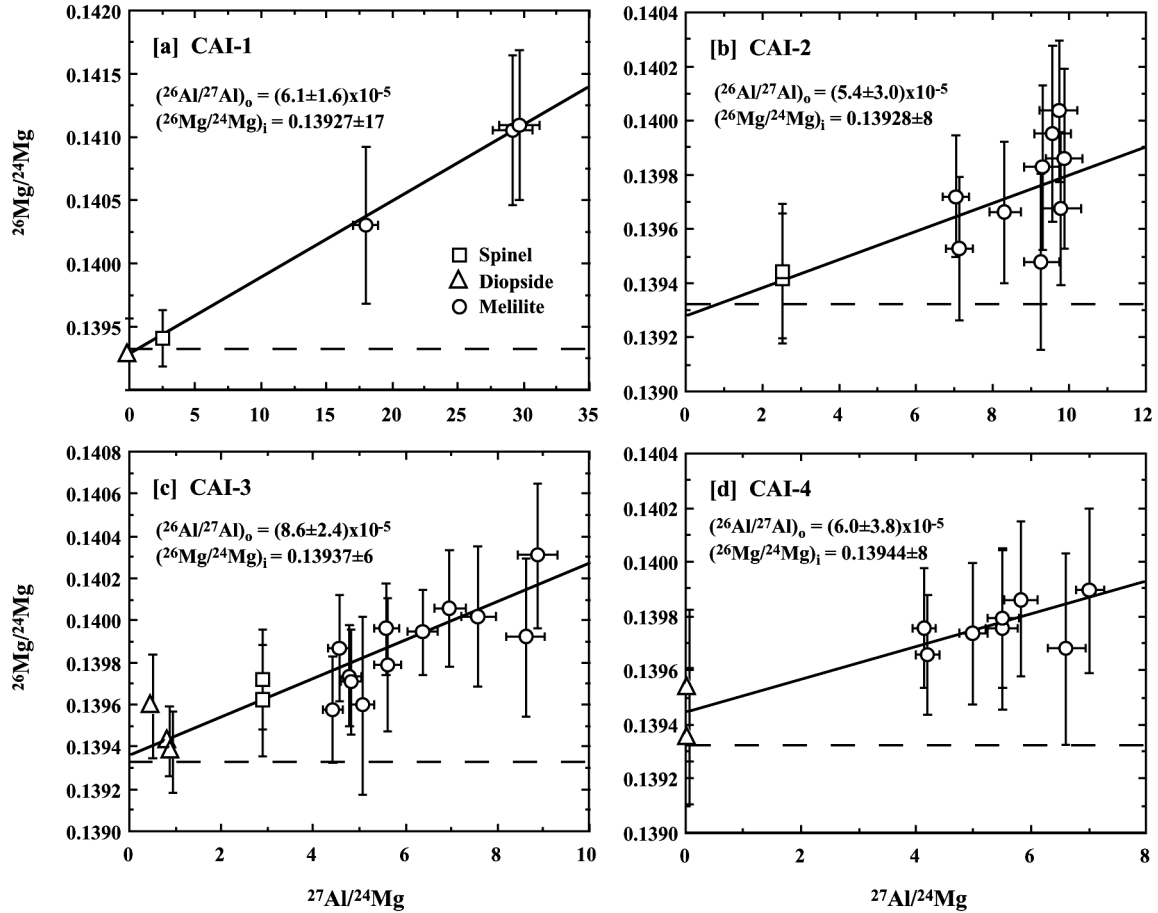


Fig. 4. $^{27}\text{Al}/^{24}\text{Mg}$ versus $^{26}\text{Mg}/^{24}\text{Mg}$ for 4 CAIs from Ningqiang. Errors plotted are 2σ mean. Terrestrial $^{26}\text{Mg}/^{24}\text{Mg}$ ratio is represented by a dashed line. The good correlation of $^{27}\text{Al}/^{24}\text{Mg}$ and $^{26}\text{Mg}/^{24}\text{Mg}$ implies in situ decay of ^{26}Al , and the inferred slope of the correlation corresponds to the initial $^{26}\text{Al}/^{27}\text{Al}$ ratio for the object: a) CAI-1 shows an excellent correlation between $^{27}\text{Al}/^{24}\text{Mg}$ (up to 30), and ^{26}Mg excess and yields $(^{26}\text{Al}/^{27}\text{Al})_0 \approx 6 \times 10^{-5}$; b) CAI-2; c) CAI-3; and d) CAI-4 also show good correlations between $^{27}\text{Al}/^{24}\text{Mg}$ and ^{26}Mg excesses. But the $^{27}\text{Al}/^{24}\text{Mg}$ ratios in these CAIs are relatively low (<10). The inferred $(^{26}\text{Al}/^{27}\text{Al})_0$ for these CAIs are 5.4×10^{-5} , 8.6×10^{-5} , and 6×10^{-5} , respectively. These values are close to the canonical values within analytical uncertainties.

DISCUSSION

Extensive searches for evidence of live ^{26}Al have been carried out in refractory inclusions from CV3 chondrites (see review of MacPherson, Davis, and Zinner 1995). Data have been collected for refractory inclusions in Allende, Leoville, Vigarano, Efremovka, Acfer 082, Grosnaja, Kaba, and more recently, Axtell. Refractory inclusions from these meteorites fall into three categories. The majority of Type A and Type B CAIs contain clear radiogenic ^{26}Mg excesses that correspond to $(^{26}\text{Al}/^{27}\text{Al})_0 \approx 5 \times 10^{-5}$. Some of these CAIs show evidence of secondary isotopic disturbance. A few CAIs formed with very little ^{26}Al . These include the FUN inclusions (named for Fractionation and Unidentified Nuclear effects; Wasserburg, Lee, and Papanastassiou 1977), which have nonradiogenic nuclear anomalies in many elements, and a handful of other unusual inclusions (e.g., Ireland, Fahey, and Zinner 1991; Russell et al. 1998). The third group of refractory inclusions

are plagioclase-olivine-bearing objects (variously called Type C CAIs, POIs, or aluminum-rich chondrules). Evidence of live ^{26}Al in these objects is limited. Sheng, Hutcheon, and Wasserburg (1991) studied 20 POIs, 17 from Allende, and one each from Adelaide, Leoville, and Vigarano. Most of them contain no evidence for $^{26}\text{Mg}^*$, but two POIs from Allende show small enrichments in ^{26}Mg that correspond to $(^{26}\text{Al}/^{27}\text{Al})_0 = 0.61 \times 10^{-5}$ and 0.26×10^{-5} . Of the four aluminum-rich chondrules from Axtell (CV3) studied by Srinivasan, Huss, and Wasserburg (2000), only one showed a resolved $^{26}\text{Mg}^*$ with an inferred $(^{26}\text{Al}/^{27}\text{Al})_0 = (0.34 \pm 0.15) \times 10^{-5}$. Marhas et al. (2000) found one anorthite-rich chondrule in Allende with a $(^{26}\text{Al}/^{27}\text{Al})_0 = 0.3 \times 10^{-5}$ and one from Efremovka with 1×10^{-5} , although other objects showed no evidence of ^{26}Al . Hutcheon, Krot, and Ulyanov (2000) also found an Al-rich chondrule in Efremovka with $(^{26}\text{Al}/^{27}\text{Al})_0 = (0.55 \pm 0.33) \times 10^{-5}$. It is probable that metamorphic heating at some stage (possibly prior to the final aggregation of the

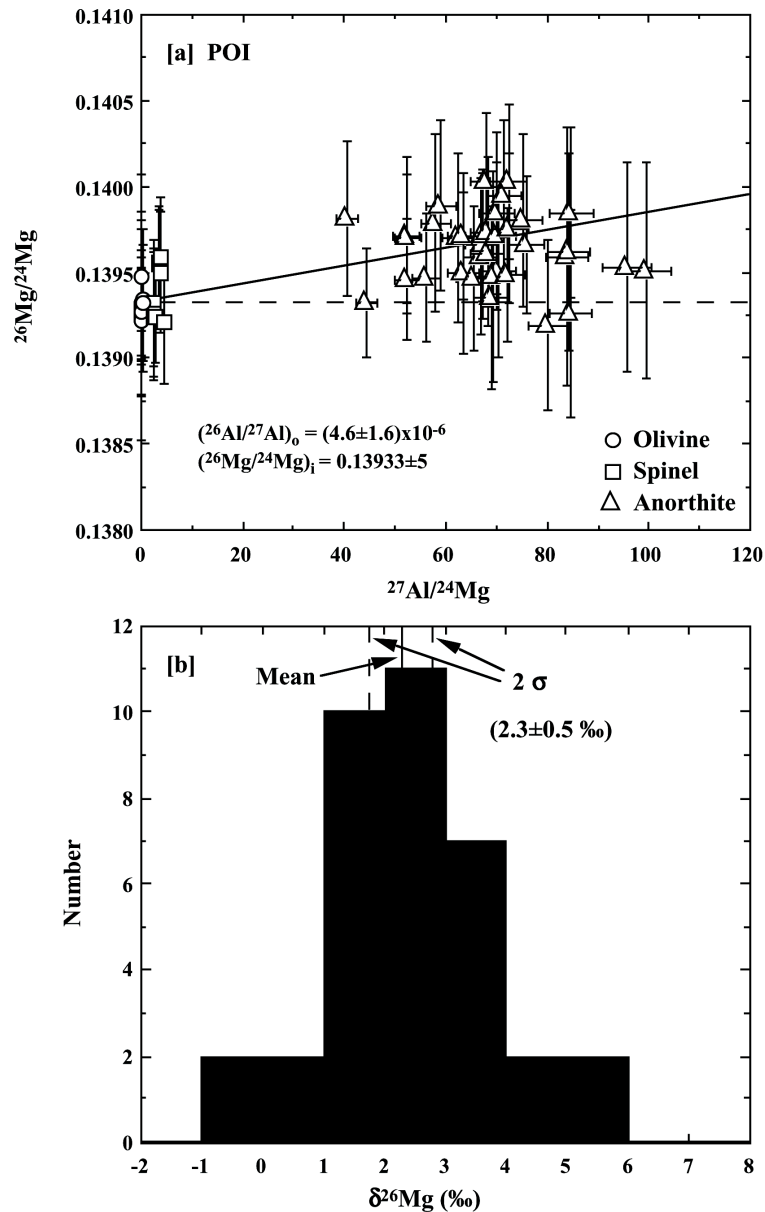


Fig. 5. a) $^{27}\text{Al}/^{24}\text{Mg}$ versus $^{26}\text{Mg}/^{24}\text{Mg}$ for the POI from Ningqiang. Anorthite has various $^{27}\text{Al}/^{24}\text{Mg}$ ratios and shows different degrees of ^{26}Mg excesses, ranging from normal to small but clear ^{26}Mg excesses (up to 5%). Spinel grains within anorthite crystals, and olivine and spinel grains between anorthite laths, have normal magnesium composition. The inferred $(^{26}\text{Al}/^{27}\text{Al})_0$ for this POI is $(4.6 \pm 1.6) \times 10^{-6}$. The regression line intercepts at the zero point with $\delta^{26}\text{Mg}$ of $0.07 \pm 0.37\%$; b) Histograms of $^{26}\text{Mg}/^{24}\text{Mg}$ measurements for anorthite of the POI. The weighted mean ($2.3 \pm 0.5\%$) of the analyses is clearly resolved from terrestrial magnesium by more than 8σ .

meteorite) has disturbed the aluminum-magnesium systematics of many plagioclase-bearing objects in CV3 chondrites (e.g., Huss et al. 2001).

The pre-metamorphic characteristics of refractory inclusions and chondrules from CV3 chondrites can be generalized to most other chondrite classes. Most commonly, Type A and Type B CAIs from carbonaceous chondrites, UOCs, and unequilibrated enstatite chondrites (UECs) have inferred $(^{26}\text{Al}/^{27}\text{Al})_0 \approx 5 \times 10^{-5}$ (Fahey et al. 1987; Russell et al. 1996; Russell et al. 1998; Guan et al. 2000). Two aluminum-

rich chondrules from Acfer 094, an anomalous but primitive C chondrite, had $(^{26}\text{Al}/^{27}\text{Al})_0 \sim 1 \times 10^{-5}$ (Hutcheon, Krot, and Ulyanov 2000). Essentially, all aluminum-rich and ferromagnesian chondrules from Type 3.0–3.1 UOCs contained ^{26}Al with $(^{26}\text{Al}/^{27}\text{Al})_0$ ratios between $\sim 0.3 \times 10^{-5}$ to $\sim 2.3 \times 10^{-5}$ (Kita et al. 2000; McKeegan et al. 2000; Huss et al. 2001; Mostefaoui et al. 2002). Most recently, an anorthite-bearing chondrule from the EH chondrite Sahara 97072 was shown to have formed with $(^{26}\text{Al}/^{27}\text{Al})_0 = (0.67 \pm 0.27) \times 10^{-5}$ (Guan et al. 2002). Thus, refractory objects and chondrules

from many classes of meteorites exhibit the same type of aluminum-magnesium isotope systematics. The CAIs typically show $(^{26}\text{Al}/^{27}\text{Al}) \sim 5 \times 10^{-5}$ (with some very low values) while POIs and ferromagnesian chondrules and Al-rich chondrules always show much lower values than 5×10^{-5} . This pattern is also found in Ningqiang. All four melilite-bearing CAIs that we studied contain clear $^{26}\text{Mg}^*$ that correspond to inferred $(^{26}\text{Al}/^{27}\text{Al})_0 \approx 10^{-5}$. Some of the $(^{26}\text{Al}/^{27}\text{Al})_0$ ratios appear to be slightly higher. However, the uncertainties are large due to the low Al/Mg ratios in melilite, and in three of four cases, the inferred $(^{26}\text{Al}/^{27}\text{Al})_0$ values are within the 2σ uncertainties of 5×10^{-5} . The fourth is within 3σ . There have been no unambiguous measurements of initial ratios higher than 5×10^{-5} in any CAI from any meteorite. We do not feel that the current data provide convincing evidence of an initial ratio higher than 5×10^{-5} in CAIs or chondrules. The correlations between ^{26}Mg excess and $^{27}\text{Al}/^{24}\text{Mg}$ in CAIs suggest that the isotope systematics in Ningqiang CAIs have not been disturbed seriously by secondary metamorphism (Fig. 4). If the parent body of Ningqiang had been significantly metamorphosed, it would not have preserved $^{26}\text{Mg}^*$ in plagioclase, melilite, and glasses. The diffusion coefficients for magnesium in plagioclase (LaTourrette and Wasserburg 1998) and melilite (LaTourrette and Hutcheon 1999) require that heating of the Ningqiang parent body was not significant.

CAI populations differ in size and mineralogy from one meteorite class to another (e.g., MacPherson, Wark, and Armstrong 1988; Russell et al. 1998; Guan et al. 2000). The population of CAIs in Ningqiang differs from that in most CV chondrites. CAIs in CV chondrites are generally abundant and large in size, ranging from mm up to cm. Most CAIs in Ningqiang are small, only up to several hundred μm (Rubin et al. 1988; Kimura et al. 1997; this work), and their modal abundance is quite low (~ 1 vol%) compared to that of CV chondrites (e.g., ~ 10 vol% in Allende; Kornacki and Wood 1984). Among the five thin sections (~ 4 cm²) we studied, only four CAIs were found corresponding to a modal abundance of 0.1 vol% (cf., $1.0_{-0.5}^{+1.0}$ vol%, Rubin et al. 1988). In spite of these differences, the Al-Mg isotope systematics of CAIs in Ningqiang are essentially identical to those found in other meteorite types.

The Ningqiang POI also shows small but significant $^{26}\text{Mg}^*$ (Fig. 5b) with an inferred $(^{26}\text{Al}/^{27}\text{Al})_0 \approx (0.46 \pm 0.16) \times 10^{-5}$. This is in line with those observed in POIs from Allende and Axtell and in anorthite-rich chondrules in other carbonaceous chondrites (Sheng, Hutcheon, and Wasserburg 1991; Hutcheon, Krot, and Ulyanov 2000; Marhas et al. 2000; Srinivasan, Huss, and Wasserburg 2000). The degree and possible effects of metamorphism of Ningqiang will be discussed below. Independent of possible secondary metamorphism, the Ningqiang POI is clearly the result of multiple stages of melting. In some previous studies, it has been possible to clearly establish the presence of earlier phases (e.g., spinels) that had distinctly different F_{Mg} values than the bulk of

the inclusion (e.g., Sheng, Hutcheon, and Wasserburg 1991). The difference found in the Ningqiang POI between F_{Mg} for spinel and for olivine and plagioclase appear to be sufficiently large to permit us to conclude that the spinels are a precursor phase made in a separate process and incorporated into the POI melt. This is supported by the rounded morphology of the spinel grains that may be attributed to resorption. This phenomenon was first discovered in a POI by Sheng, Hutcheon, and Wasserburg (1991), who found clear evidence of spinel resorption and who also demonstrated the phase relationships and cooling rates necessary to achieve preservation of the spinel precursor phase. Lin and Kimura (1997) noted that spinels in Ningqiang POIs contain much lower Cr_2O_3 than what is expected if this mineral crystallized from a melt with its bulk Cr_2O_3 content. A relict origin was then suggested for spinel in Ningqiang POIs (Lin and Kimura 1997). It now appears to be a common phenomenon that POIs, some CAIs, and some chondrules formed from melt droplets that incorporated debris from earlier crystallization processes, available in the local environment where the POIs formed. The POIs are clearly the product of incomplete melting and the reaction of precursor crystals engulfed in a silicate melt followed by crystallization of the melt. They are not aggregates. The demonstration of variable fractionation factors for Mg in different minerals in some CAIs (including fine-grained CAIs) and POIs has been observed many times (cf., Sheng, Hutcheon, and Wasserburg 1991; Brigham 1990). The role of multi-stage formation and reprocessing must therefore be included in models that seek to explain these objects.

Two ferromagnesian chondrules in Ningqiang exhibit resolved ^{26}Mg excess. Their inferred $(^{26}\text{Al}/^{27}\text{Al})_0$ ratios are one order of magnitude lower than 5×10^{-5} , but are consistent with the data observed in aluminum-rich chondrules from unequilibrated carbonaceous, enstatite, and ordinary chondrites and in ferromagnesian chondrules from UOCs (Sheng, Hutcheon, and Wasserburg 1991; Russell et al. 1996; Srinivasan, Huss, and Wasserburg 2000; Kita et al. 2000; McKeegan et al. 2000; Guan et al. 2002; Mostefaoui et al. 2002). Among CV chondrites, only a relatively small fraction of aluminum-rich chondrules contain detectable $^{26}\text{Mg}^*$ (e.g., Sheng, Hutcheon, and Wasserburg 1991; Srinivasan, Huss, and Wasserburg 2000). It is possible that this is due to metamorphism of the host meteorites. Allende and Axtell, oxidized CV3 chondrites, have presolar grains populations that suggest metamorphic temperatures of 550–600°C (Huss and Lewis 1994; Huss, Meshik, Hohenberg 2000). Such temperatures are sufficient to homogenize the magnesium isotopic compositions of 50 μm anorthite crystals or of melilite on time scales of 10^6 years (LaTourrette and Wasserburg 1998; LaTourrette and Hutcheon 1999). We note that the diffusion rates in glasses are typically much greater than for the corresponding crystalline phases (cf., Sheng, Hutcheon, and Wasserburg 1991). We therefore expect that the mesostasis would have almost completely equilibrated in

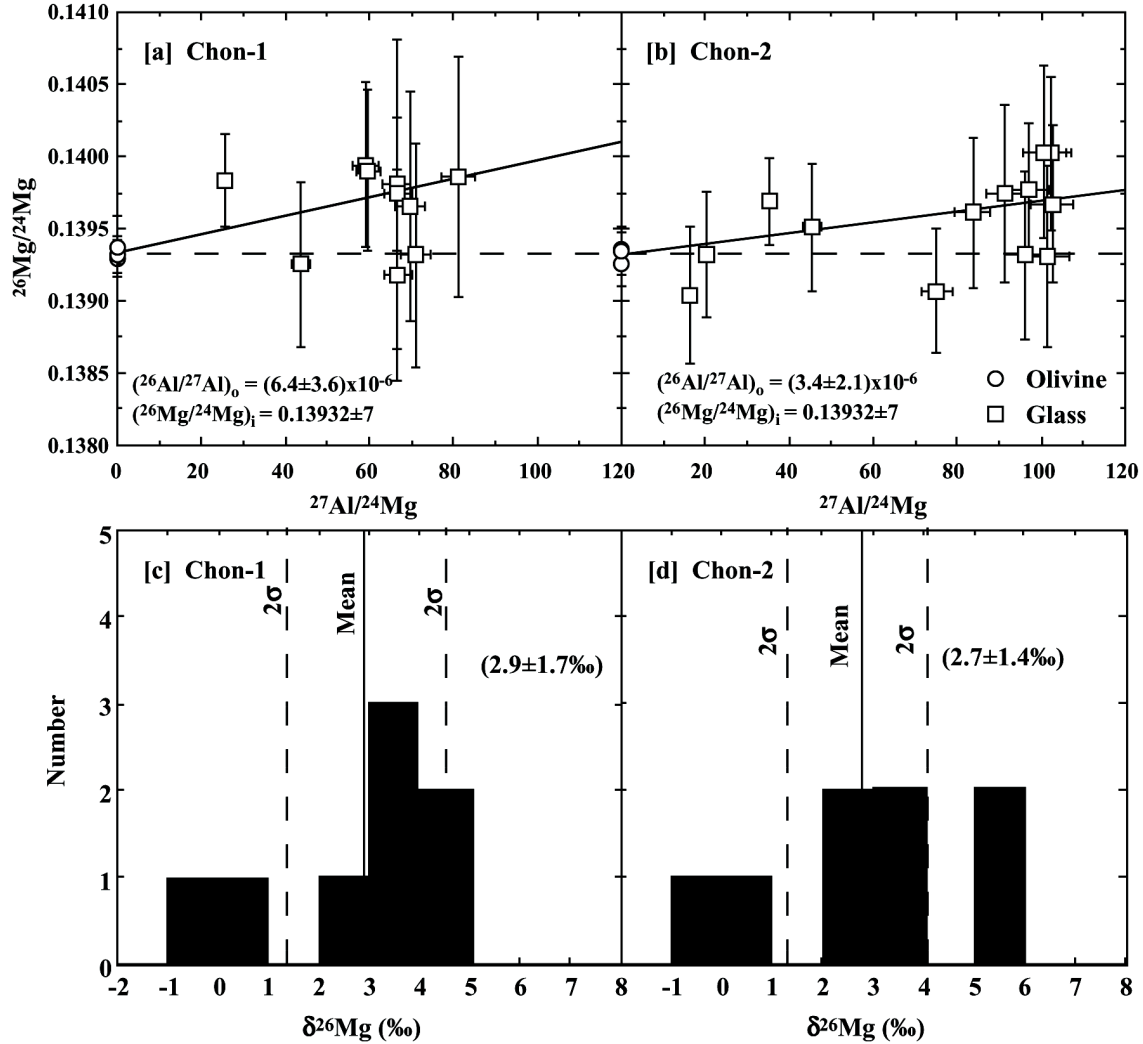


Fig. 6. (a) and (b) $^{27}\text{Al}/^{24}\text{Mg}$ versus $^{26}\text{Mg}/^{24}\text{Mg}$ for two olivine chondrules from Ningqiang. The major phase, olivine, has normal magnesium isotopic compositions relative to terrestrial standards. But the aluminum-rich glass in the chondrules show various degrees of ^{26}Mg excess (up to 5‰). The inferred $(^{26}\text{Al}/^{27}\text{Al})_0$ for these two ferromagnesian chondrules are 6.4×10^{-6} and 3.4×10^{-6} . The regression lines intercept at the zero point with ^{26}Mg of $0.03 \pm 0.52\%$ and $0.01 \pm 0.50\%$, respectively for Chon-1 and Chon-2. (c) and (d) Histograms of $^{26}\text{Mg}/^{24}\text{Mg}$ measurements for Al-rich glass with $^{27}\text{Al}/^{24}\text{Mg} > 60$ and 80, respectively in chondrules Chon-1 and Chon-2. The weighted means of the analyses are clearly resolved from terrestrial magnesium by more than 3σ .

chondrules with small effects on plagioclase and melilite. However, this would not be the case for plagioclase in the POIs. Some of the CAIs in both Allende and Axtell show evidence of disturbance in the aluminum-magnesium isotopic system (Podosek et al. 1991, Srinivasan, Huss, and Wasserburg 2000). Efremovka, a reduced CV3.2 chondrite, may have only seen metamorphic temperatures of 400–450°C (cf., Huss and Lewis 1994). The CAIs in Efremovka may be less disturbed than those in Allende, although minor disturbances are evident in some inclusions (Goswami, Srinivasan, and Ulyanov 1994). In addition, aluminum-rich chondrules from Efremovka contain a larger fraction of detectable $^{26}\text{Mg}^*$ than similar chondrules from Allende and Axtell.

To what extent has metamorphism affected Ningqiang? A petrological study of Ningqiang suggested an equilibration temperature of 300°C using cobalt partitioning between cobalt-rich metal and awaruite (Kimura et al. 1997). An independent thermoluminescence study yielded a similar result (Guimon et al. 1995). At this temperature, magnesium isotopes in melilite and anorthite would not be equilibrated with Mg rich phases over the age of the solar system. Our Mg-Al data also support a low degree of thermal metamorphism for Ningqiang. We found that melilite grains as small as 10 μm in some CAIs contain clear $^{26}\text{Mg}^*$ excesses. Had Ningqiang experienced high temperature (>525°C) metamorphism for 4×10^5 years in its parent body, $^{26}\text{Mg}^*$ excesses would have been completely erased in these small

melilite and anorthite grains. If the temperature of 475°C had been maintained for 7×10^6 years, it would also have erased the isotopic effects in magnesium (LaTourrette and Wasserburg 1998). It is reasonable to conclude that aluminum-magnesium systematics in Ningqiang have not been seriously affected by thermal metamorphism in its parent body and that the magnesium isotopes of CAIs, POI, and chondrules in Ningqiang must reflect the values at the time of incorporation into the parent body. Therefore, the ^{26}Al isotopic effects, including the distinctive differences between CAIs, chondrules, and the POI, must reflect the pre-accretionary history (i.e., prior to forming the Ningqiang parent body). It is very reasonable that the debris which was accumulated to form the chondrite represented materials with widely different igneous and metamorphic histories.

In summary, the low level of metamorphism in Ningqiang has preserved evidence of ^{26}Al in 4 CAIs, 1 POI, and 2 chondrules. The initial ratios for the Ningqiang CAIs are consistent with those found in most CAIs from unequilibrated C, E, and O chondrites. The ratios for the Ningqiang POI and chondrules are similar to those found in similar objects from the least metamorphosed C, E, and O chondrite. A consistent pattern has emerged from several studies. Many CAIs from all classes of chondrites typically had ^{26}Al at $(^{26}\text{Al}/^{27}\text{Al})_0 \approx 5 \times 10^{-5}$ when they formed, and some had much less. In contrast, POIs, aluminum-rich chondrules, and ferromagnesian chondrules formed with initial ratios 5–10 times lower. This consistency implies broad-scale homogeneity in ^{26}Al in the chondrite-forming region of the nebula. The differences in initial ratios between CAIs and less-refractory objects in unmetamorphosed chondrites can be interpreted either in terms of formation times, times of secondary alteration, or in terms of initial differences in ^{26}Al abundance (at the same time) in the regions where the objects formed (nebular heterogeneity). Huss et al. (2001) give a detailed discussion of the different possible interpretations of the ^{26}Al data. We find that the consistency of the data across chondrite classes can most plausibly be explained by a ~ 2 million year time difference between the formation of CAIs and the onset of formation of less refractory objects. This model requires that some CAIs were formed late or were reformed late. This problem of late formation of CAIs has not been addressed and remains an important issue.

CONCLUSIONS

Four CAIs from Ningqiang were found to contain excesses of ^{26}Mg . These excesses correlate reasonably well with Al/Mg, and are attributed to the in situ decay of ^{26}Al . The $(^{26}\text{Al}/^{27}\text{Al})_0$ ratios found for these CAIs are within the quoted uncertainties equal to $^{26}\text{Al}/^{27}\text{Al} = 5 \times 10^{-5}$. These results extend those of previous workers showing that CAIs with $(^{26}\text{Al}/^{27}\text{Al})_0 \approx 5 \times 10^{-5}$ were widespread in all classes of

chondrites. There is no convincing evidence of ratios higher than this value for materials processed in the solar system, but there is abundant evidence of CAIs with $(^{26}\text{Al}/^{27}\text{Al})_0$ less than this value. This behavior in CAIs is grossly distinct from that found for $^{26}\text{Al}/^{27}\text{Al}$ in preserved presolar oxide grains, which show an enormous range in $^{26}\text{Al}/^{27}\text{Al}$ ratios (from less than 10^{-5} to 10^{-2}).

A POI was found with clear evidence of $^{26}\text{Mg}^*$ in plagioclase and normal magnesium in spinel and olivine. For this POI, the inferred $(^{26}\text{Al}/^{27}\text{Al})_0$ is $(0.46 \pm 0.16) \times 10^{-5}$. This is in accord with the values found for some similar objects in other carbonaceous chondrites (e.g., Sheng, Hutcheon, and Wasserburg 1991; Srinivasan, Huss, and Wasserburg 2000; Hutcheon, Krot, and Ulyanov 2000). The POI studied here contains rounded spinel crystals with $^{25}\text{Mg}/^{24}\text{Mg}$ that is distinctly fractionated compared to the other phases in the POI. This and earlier observations demonstrate that these objects contain relict grains produced by previous and distinctly separate generations of activity (cf., Sheng, Hutcheon, and Wasserburg 1991; Srinivasan, Huss, and Wasserburg 2000).

Two chondrules were found to contain glasses with sufficiently high Al/Mg to justify a search for $^{26}\text{Mg}^*$. Excesses of $^{26}\text{Mg}^*$ were found in the glasses, while olivine in both chondrules had normal magnesium. The excesses are interpreted to be due to in situ decay of ^{26}Al from $(^{26}\text{Al}/^{27}\text{Al})_0$ values of $0.3\text{--}0.6 \times 10^{-5}$. Again, these values are consistent with those found in chondrules from other classes of chondrites (e.g., Kita et al. 2001; Huss et al. 2001).

These observations support the view that ^{26}Al was widely and approximately homogeneously distributed throughout the condensed matter of the solar system. The difference in $(^{26}\text{Al}/^{27}\text{Al})_0$ between CAIs and less refractory materials seems best interpreted in terms of a ~ 2 million yr delay between the formation of CAIs and the onset of the formation of less refractory objects. Models that attempt to explain the observations in terms of a grossly heterogeneous initial distribution of ^{26}Al cannot easily explain the ^{26}Al systematics found in Ningqiang and other primitive chondrites. However, the presence of CAIs with very low ^{26}Al is not yet explained. If $(^{26}\text{Al}/^{27}\text{Al}) = 5 \times 10^{-5}$ was characteristic of condensed solar system matter, then this requires that the process that produced CAIs continued late or that these objects were metamorphosed late.

Acknowledgments—The thin section containing the POI was kindly provided by Dr. Alan Rubin. We appreciate the critical and constructive comments of the reviewers, J. Goswami and N. T. Kita. Their suggestions as well as the thorough and helpful comments by the associate editor, H. Nagahara, have been incorporated to provide a better presentation. This study was supported by NASA NAG5-10293 (GJW) and NAG5-8158 (GRH) and Caltech Division Contribution #8738(1069).

REFERENCES

- Brigham C. A. 1990. Isotopic heterogeneity in calcium-aluminum-rich meteoritic inclusions. Ph.D. thesis, California Institute of Technology, Pasadena, California, USA.
- Catanzaro E. J., Murphy T. J., Garner E. L., and Shields W. R. 1966. Absolute isotopic abundance ratios and atomic weights of magnesium. *Journal of Research of the National Bureau of Standards* 70a:453–458.
- Fahey A., Goswami J. N., McKeegan K. D., and Zinner E. 1987. ^{26}Al , ^{244}Pu , ^{50}Ti , REE, and trace element abundances in hibonite grains from CM and CV meteorites. *Geochimica et Cosmochimica Acta* 51:329–350.
- Goswami J. N., Srinivasan G., and Ulyanov A. A. 1994. Ion microprobe studies of Efremovka CAIs: I. Magnesium isotope composition. *Geochimica et Cosmochimica Acta* 58:431–447.
- Guan Y., Huss G. R., MacPherson G. J., and Wasserburg G. J. 2000. Calcium-aluminum-rich inclusions from enstatite chondrites: Indigenous or foreign? *Science* 289:1330–1333.
- Guan Y., Huss G. R., MacPherson G. J., and Leshin L. A. 2002. Aluminum-magnesium isotope systematics of aluminum-rich chondrules in unequilibrated enstatite chondrites (abstract #2034). 33rd Lunar and Planetary Science Conference. CD-ROM.
- Guimon R. K., Symes S. J. K., Sears D. W. G., and Benoit P. H. 1995. Chemical and physical studies of type 3 chondrites XII: The metamorphic history of CV chondrites and their components. *Meteoritics* 30:704–714.
- Hsu W., Huss G. R., and Wasserburg G. J. 1999. An ion probe study of Al-Mg systematics in the Ningqiang carbonaceous chondrite (abstract #1488). 30th Lunar and Planetary Science Conference. CD-ROM.
- Hsu W., Wasserburg G. J., and Huss G. R. 2000. High time resolution by use of the ^{26}Al chronometer in the multistage formation of a CAI. *Earth and Planetary Science Letters* 182:15–29.
- Huss G. R. and Lewis R. S. 1994. Noble gases in presolar diamonds II: Component abundances reflect thermal processing. *Meteoritics* 29:811–829.
- Huss G. R., Meshik A. P., and Hohenberg C. M. 2000. Abundances of presolar grains in Renazzo and Axtell: Implications for their thermal histories (abstract #1467). 31st Lunar and Planetary Science Conference. CD-ROM.
- Huss G. R., MacPherson G. J., Wasserburg G. J., Russell S. S., and Srinivasan G. 2001. Aluminum-26 in calcium-aluminum-rich inclusions and chondrules from unequilibrated ordinary chondrites. *Meteoritics & Planetary Sciences* 36:975–997.
- Hutcheon I. D. and Hutchison R. 1989. Evidence from the Semarkona ordinary chondrite for ^{26}Al heating of small planets. *Nature* 337:238–241.
- Hutcheon I. D., Krot A. N., and Ulyanov A. A. 2000. ^{26}Al in anorthite-rich chondrules in primitive carbonaceous chondrites: Evidence chondrules postdate CAI (abstract #1869). 31st Lunar and Planetary Science Conference. CD-ROM.
- Ireland T. R., Fahey A. J., and Zinner E. K. 1991. Hibonite-bearing microspherules: A new type of refractory inclusions with large isotopic anomalies. *Geochimica et Cosmochimica Acta* 55:367–379.
- Kallemeyn G. M. 1996. The classificational wanderings of the Ningqiang chondrite (abstract). 27th Lunar and Planetary Science Conference. pp. 635–636.
- Kimura M., Noguchi T., Lin Y., and Wang D. 1997. Petrology and mineralogy of an unusual Ningqiang carbonaceous chondrite. In *Geochemical studies on synthetic and natural rock systems*, edited by Gupta A. K., Onuma K., and Arima M. Chennai: Allied Publishers Ltd. pp. 153–165.
- Kita N. T., Nagahara H., Togashi S., and Morishita Y. 2000. A short duration of chondrule formation in the solar nebula: Evidence from ^{26}Al in Semarkona ferromagnesian chondrules. *Geochimica et Cosmochimica Acta* 64:3913–3922.
- Kornacki A. S. and Wood J. A. 1984. Petrography and classification of Ca, Al-rich, and olivine-rich inclusions in the Allende CV3 chondrite. Proceedings, 14th Lunar and Planetary Science Conference. *Journal of Geophysical Research* 89:B573–B587.
- LaTourrette T. and Wasserburg G. J. 1998. Magnesium diffusion in anorthite: Implications for the formation of early solar system planetesimals. *Earth and Planetary Science Letters* 158:91–108.
- LaTourrette T. and Hutcheon I. D. 1999. Magnesium diffusion in melilite: Thermal histories for CAIs and their parent bodies (abstract #2003). 30th Lunar and Planetary Science Conference. CD-ROM.
- Lee T., Papanastassiou D. A., and Wasserburg G. J. 1976. Demonstration of ^{26}Mg excess in Allende and evidence for ^{26}Al . *Geophysical Research Letters* 3:109–112.
- Lee T., Papanastassiou D. A., and Wasserburg G. J. 1977. ^{26}Al in the early solar system: Fossil or fuel? *Astrophysical Journal Letters* 211:L107–L110.
- Lin Y. and Kimura M. 1997. Titanium-rich, oxide-bearing plagioclase-olivine inclusions in the unusual Ningqiang carbonaceous chondrite. *Antarctic Meteorite Research* 10:227–248.
- MacPherson G. J., Wark D. A., and Armstrong J. T. 1988. Primitive material surviving in chondrites: Refractory inclusions. In *Meteorites and the early solar system*, edited by Kerridge J. F. and Mathews M. S. Tucson: University of Arizona Press. pp. 746–807.
- MacPherson G. J., Davis A. M., and Zinner E. K. 1995. The distribution of aluminum-26 in the early solar system—A reappraisal. *Meteoritics* 30:365–386.
- Marhas K. K., Hutcheon I. D., Krot A. N., Goswami J. N., Komatsu M. 2000. Aluminum-26 in carbonaceous chondrite chondrules. *Meteoritics & Planetary Science* 35:A102.
- McKeegan K. D., Greenwood J. P., Leshin L., and Cosarinsky M. 2000. Abundance of ^{26}Al in ferromagnesian chondrules of unequilibrated ordinary chondrites (abstract #2009). 31st Lunar and Planetary Science Conference. CD-ROM.
- Mostefaoui S., Kita N. T., Togashi S., Tachibana S., Nagahara H., and Morishita Y. 2002. The relative formation ages of ferromagnesian chondrules inferred from their initial aluminum-26/aluminum-27 ratios. *Meteoritics & Planetary Science* 37:21–438.
- Podosek F. A., Zinner E. K., MacPherson G. J., Lundberg L. L., Brannon J. C., and Fahey A. J. 1991. Correlated study of initial $^{87}\text{Sr}/^{86}\text{Sr}$ and Al-Mg isotopic systematics and petrologic properties in a suite of refractory inclusions from the Allende meteorite. *Geochimica et Cosmochimica Acta* 55:1083–1110.
- Rubin A., Wang D., Kallemeyn G., and Wasson J. 1988. The Ningqiang meteorite: Classification and petrology of an anomalous CV chondrite. *Meteoritics* 23:13–23.
- Russell S. S., Srinivasan G., Huss G. R., Wasserburg G. J., and MacPherson G. J. 1996. Evidence for widespread ^{26}Al in the solar nebula and constraints for nebula time scales. *Science* 273:757–762.
- Russell S. S., Huss G. R., Fahey A. J., Greenwood R. C., Hutchison R., and Wasserburg G. J. 1998. An isotopic and petrologic study of calcium-aluminum-rich inclusions from CO3 meteorites. *Geochimica et Cosmochimica Acta* 62:689–714.
- Sheng Y. J., Hutcheon I. D., and Wasserburg G. J. 1991. Origin of plagioclase-olivine inclusions in carbonaceous chondrites. *Geochimica et Cosmochimica Acta* 55:581–599.
- Srinivasan G., Huss G. R., and Wasserburg G. J. 2000. A petrographic,

- chemical, and isotopic study of calcium-aluminum-rich inclusions and aluminum-rich chondrules from the Axtell (CV3) chondrite. *Meteoritics & Planetary Sciences* 35:1333–1354.
- Wasserburg G. J., Lee T., and Papanastassiou D. A. 1977. Correlated oxygen and magnesium isotopic anomalies in Allende inclusions: II. Magnesium. *Geophysical Research Letters* 4:299–302.
- Wasserburg G. J. and Papanastassiou D. A. 1982. Some short-lived nuclides in the early solar system—A connection with the placental ISM. In *Essays in nuclear astrophysics*, edited by Barnes C. A. New York: Cambridge University Press. pp. 77–140.
- Weisberg M. K., Prinz M., Zolensky M. E., Clayton R. N., Mayeda T. K., and Ebihara M. 1996. Ningqiang and its relationship to oxidized CV3 chondrites (abstract). *Meteoritics & Planetary Science* 31:A150–A151.
-